# Influence of substrate miscut angle on surface morphology and luminescence properties of AlGaN

Gunnar Kusch,[1,a)] Haoning Li,[2,3] Paul R. Edwards,[1] Jochen Bruckbauer,[1] Thomas C. Sadler,[2] Peter J. Parbrook,[2,3] and Robert W. Martin[1]
[1]*Department of Physics, SUPA, University of Strathclyde, Glasgow G4 0NG, United Kingdom*
[2]*Tyndall National Institute, University College Cork, Lee Maltings, Dyke Parade, Cork, Ireland*
[3]*School of Engineering, University College Cork, College Road, Cork, Ireland*

(Received 18 December 2013; accepted 17 February 2014; published online 6 March 2014)

The influence of substrate miscut on $Al_{0.5}Ga_{0.5}N$ layers was investigated using cathodoluminescence (CL) hyperspectral imaging and secondary electron imaging in an environmental scanning electron microscope. The samples were also characterized using atomic force microscopy and high resolution X-ray diffraction. It was found that small changes in substrate miscut have a strong influence on the morphology and luminescence properties of the AlGaN layers. Two different types are resolved. For low miscut angle, a crack-free morphology consisting of randomly sized domains is observed, between which there are notable shifts in the AlGaN near band edge emission energy. For high miscut angle, a morphology with step bunches and compositional inhomogeneities along the step bunches, evidenced by an additional CL peak along the step bunches, are observed.  [http://dx.doi.org/10.1063/1.4867165]

There is much potential in the use of high quality AlGaN layers for multi-quantum well based UV-light emitting devices. The growth and applications of such structures have not been fully explored, and these remain one of the key challenges in the III-nitride material system. This is due to the complicated growth mechanics which potentially lead to phase separation and compositional inhomogeneity. Minimisation of these effects in the active region requires the growth of AlGaN buffer layers with high AlN content and high crystalline quality. In this paper, we investigate the influence of the substrate miscut on the optical and morphological properties of AlGaN buffer layers in order to optimize the crystalline quality of the buffer layer and reduce compositional inhomogeneity.

Obtaining optical information of wide band gap semiconductors is a challenging task. While this has been done by photoluminescence (PL), using 193 nm or 244 nm lasers, the spatial resolution of PL is too low to investigate submicron surface features. Additionally, standard PL spectroscopy setups do not allow surface imaging, thus preventing the correlation of the luminescence with surface features. Using cathodoluminescence (CL) in a secondary electron microscope (SEM) enables information to be obtained on the surface morphology and the optical properties at the same time, allowing the two properties to be correlated.[1] For near-insulating materials, it is necessary to cope with charging effects which might influence measurements or even prevent measurements at all. These effects can be reduced by using a low pressure arrangement. Here, we report the use of CL spectroscopy in a low vacuum SEM to study the effect of the substrate miscut angle on the surface morphology and luminescence properties of low conductivity, nominally $Al_{0.5}Ga_{0.5}N$ epilayers.

Two samples were grown, under the same growth conditions, at the Tyndall National Institute, on c-plane sapphire substrates with a miscut of 0.1° (A) and 0.4° (B) towards the m-plane, using an Aixtron close-coupled showerhead $3 \times 2''$ metalorganic vapour phase reactor. Trimethylgallium (TMGa), trimethylaluminium (TMAl), and ammonia ($NH_3$) were used as precursors, while the carrier gas was hydrogen ($H_2$). The samples consist of a 1 $\mu$m AlN layer grown on the sapphire substrate, followed by a 1 $\mu$m GaN layer and 2-period insertion layers of high temperature (HT)-GaN (10 nm) and low temperature (LT)-AlN (1 nm). On top of this structure, 2 $\mu$m of nominally undoped $Al_{0.5}Ga_{0.5}N$ was deposited. High resolution X-ray diffraction (HR-XRD) scans were performed to determine the composition and show an AlN content of approximately 47% for both samples. Reciprocal space maps indicate that the AlGaN layer in both samples is fully relaxed. In order to investigate the surface morphology, a FEI Quanta 250 environmental secondary electron microscope (ESEM) and atomic force microscopy (AFM) in tapping mode were used. The ESEM allows a small amount of water vapour to be introduced into the chamber; when ionised by electrons emitted from the sample surface, this acts to dissipate accumulated charge at the surface, thus allowing high resolution measurement of low conductivity samples without further preparation. Cathodoluminescence hyperspectral imaging[2,3] was conducted in the ESEM with a 1200 lines/mm grating blazed at 350 nm, a 50 $\mu$m slit, a focal length of 125 mm, and a 1600-element charge-coupled device. The measurements were performed at room temperature with an acceleration voltage of 5 kV and a beam current of 2.9 nA. At this acceleration voltage 90% of the beam energy is deposited within a depth of approximately 90 nm according to Monte Carlo simulations using CASINO software.[4] The sample is tilted by 45° with respect to the electron beam and the generated light is collected by a reflecting objective with its optical axis perpendicular to the electron beam as described by Edwards *et al.*[5] The generated data set was treated mathematically to extract information about the emission energy as well

a)gunnar.kusch@strath.ac.uk

 

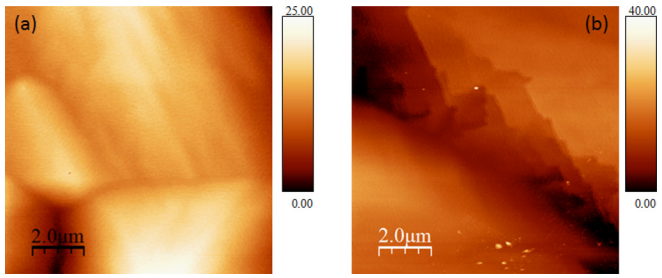


FIG. 1. AFM images of sample A (a) with a miscut of 0.1° and B (b) with a miscut of 0.4°. The different surface morphologies are clearly visible.

as the intensity of each of the peaks. For the presented analysis, each spectrum in the CL-maps was fitted using a Voigt function to generate 2D maps of the fitting parameters, such as CL peak intensity and energy.

AFM measurements over $10 \times 10\,\mu m^2$ areas (Fig. 1) show distinctive differences between the two samples. Sample A with a miscut of 0.1° shows the formation of different hillocks with an RMS roughness of 4 nm, while sample B (0.4° miscut) also shows step bunches with a height of 5 nm and an RMS roughness of 5.3 nm. Step bunches can be generated during growth on vicinal substrates where the miscut of the substrate results in the formation of a considerable number of steps. The development of a morphology from monoatomic steps to form step bunches can be driven by a number of factors, including, for example, to relieve stress from the as grown material.[6] During the growth of c-plane III-nitrides, these step edges are non c-plane facets which might locally influence the material quality. In order to investigate the surface morphology on a larger scale and probe the luminescence properties of the AlGaN layer, CL hyperspectral imaging was conducted. The measurements were performed at a chamber pressure of 0.1–0.3 millibars as measurements at high magnification (e.g. × 1 2 000) were not possible on these samples at high vacuum, due to charging effects. Secondary electron (SE) imaging of sample A in the ESEM reveals a crack-free morphology consisting of several areas with a random size and shape distribution, separated by valleys. This is consistent with measurements performed by AFM. Figs. 2(b) and 2(c) show the $10 \times 10\,\mu m^2$ maps of the fitted CL peak energy and intensity, respectively, of the AlGaN near band edge (NBE) peak, which were acquired from the centre of the SE image in Fig. 2(a). The CL energy map reveals domains between which there are notable shifts in the AlGaN NBE emission energy. For example, the energy map in Fig. 2(b) shows regions with a peak centred in between 4.58 eV and 4.53 eV. Within each domain, the peak energy remains fairly constant. Comparing this with the CL intensity map, we can observe a clear correlation between the intensity distribution and the emission energy. The intensity is highest for low emission energies and decreases with increasing energy. The variation in the emission energy could be caused by different effects. One phenomenon which could be causing both the observed morphology and luminescence is a compositional pulling effect. This effect causes a gradual compositional variation in the epitaxial layer due to compressive biaxial strain caused by the lattice mismatch between buffer and the overgrown layer,[7,8] which can lead to lateral compositional variations. Another effect might be the growth of AlGaN micro-crystallites with slightly different orientations and composition.[9] Furthermore, the large difference in the mobility of Ga and Al atoms[10] during the growth can lead to the nucleation of islands during the initial growth stage. Due to their higher mobility, Ga atoms contribute more to the growth of the islands while Al atoms are incorporated more randomly. The effect of this initial behaviour lessens with subsequent growth but can still lead to a significant AlGaN compositional inhomogeneity.[11] The first two effects are unlikely for our sample series as XRD measurements do not show any signs of micro-crystallites and the layer is expected to grow unstrained due to the 2-period insertion layers of HT-GaN and LT-AlN. Determination of which of these effects is dominant would require further measurements, such as the direct measurement of the strain using electron backscatter diffraction. If the effect is caused by a change in the composition alone, it would correspond to a decrease in the AlN content by about 2 at. %. The black features seen in the SE image of the sample are most likely defect-related but show no influence on the intensity or emission energy of the investigated area. The SE images of sample B in Figs. 3(a) and 4(a) reflect the topography in the corresponding AFM measurement in Fig. 1(b). The surface is smooth apart from large steps. The step direction follows an underlying association with the miscut orientation, while the step length varies greatly. The steps are formed during growth by step bunching. Hyperspectral CL imaging of a $10 \times 10\,\mu m^2$ area in the centre of the SE images reveals two NBE AlGaN peaks at 4.41 eV and 4.54 eV, which strongly depend on the morphology. The intensity of the 4.54 eV

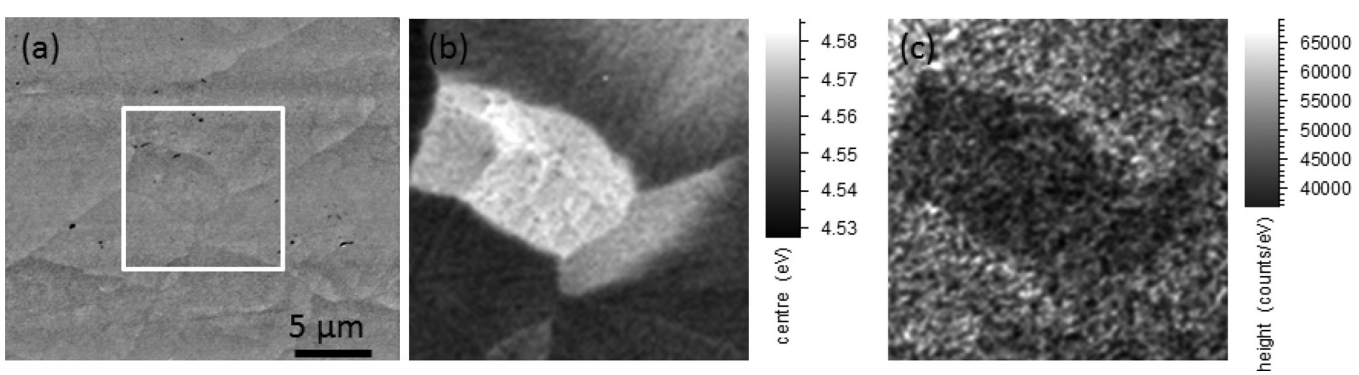


FIG. 2. SE image (a) and fitted $10 \times 10\,\mu m^2$ CL-maps of the peak energy (b) and intensity (c) of sample A.

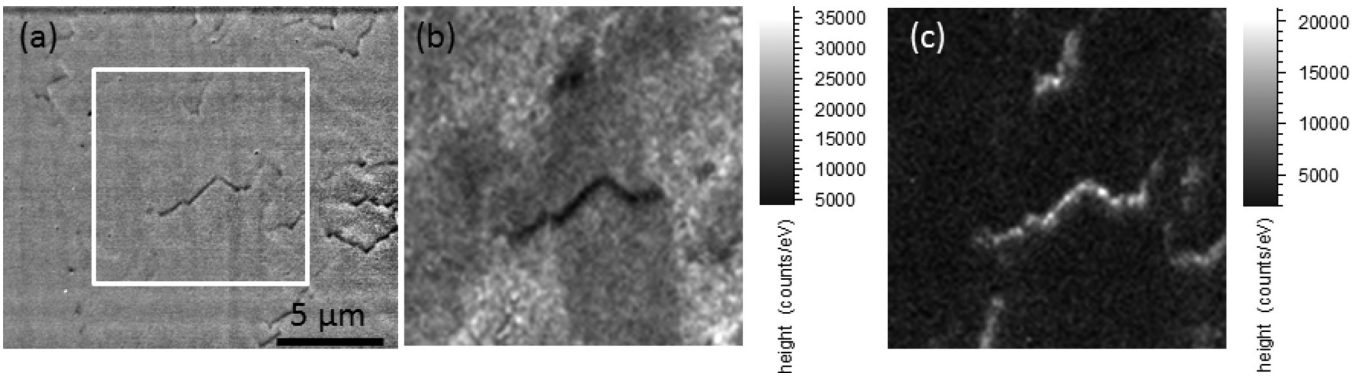


FIG. 3. SE image (a) and fitted $10 \times 10\ \mu m^2$ CL intensity maps of the 4.54 eV peak (b) and the 4.41 eV peak (c) of sample B.

peak (Fig. 3(b)) is mostly constant over the measured area with a large drop in intensity along the step edges seen in the SE image, while there is only a small variation of the emission energy over the scanned area (not shown). The 4.41 eV luminescence (Fig. 3(c)) is highly localized and occurs along the step edge. This observation is strengthened by the hyperspectral CL images taken at a higher magnification (Fig. 4) in which the intensity of the lower energy peak (Fig. 4(c)) perfectly matches the step edge imaged in the SE image. This indicates that along step edges the growth conditions of AlGaN are different than on the otherwise smooth sample surface. Comparison between the intensity maps of both peaks shows an inverse relationship. This suggests that the 4.41 eV peak is not an additional peak but instead a peak of the NBE emission of an AlGaN layer with a lower AlN content (Fig. 5). The shift in emission energy corresponds to a change in the AlN content by about 5 at. %. This behaviour was previously seen by Chang *et al.*[12] and attributed to the lower surface mobility of Al during the growth which decreases the incorporation probability of Al along step edges. The additional bright area running vertically in Fig. 4(c), which does not correlate with the SE image, is suspected to originate from an overgrown stepbunch. Direct comparison of the SE images of both samples at the same magnification (Fig. 2(a) for A and Fig. 3(a) for B) underlines the differences shown in the AFM measurement. While sample A shows the formation of domains on the surface, no such domains are present in sample B; instead step bunches can be seen on the surface. The same differences are visible in the CL peak intensity maps of both samples. These differences can be explained by the different miscut angle of the substrate: a high miscut angle promotes the formation of step bunches[13] which may be assisting in the relief of stress.[6] The formation of step edges on $Al_{0.5}Ga_{0.5}N$ has already been reported on epitaxial lateral overgrown (ELO) samples in Ref. 14. Those samples showed step bunches with a height of either 70 nm or 2–4 nm, along with a change in the composition between the flat terraces (50% AlN) and step edges (34% or 41% AlN), depending on the thickness of the AlGaN layer (0.7 $\mu$m or 3.5 $\mu$m). On the ELO samples, the non c-plane facets form during the overgrowth of the pattern etched into the substrate. The formation of the non c-plane facets in the samples presented in this paper is due to the miscut of the substrate. The step bunches seen in the 0.7 $\mu$m thick sample in Ref. 14 are continuous and their spacing and direction are aligned with the underlying ELO pattern. The step bunches seen in our investigation and their 3.5 $\mu$m thick sample are of varying length and exhibit a zigzag pattern with the main orientation following the underlying ELO pattern or miscut orientation, respectively.

We have demonstrated that combining CL hyperspectral imaging with the capabilities of an ESEM allows the technique to be extended to the characterisation of low conductivity materials. It allows correlation of the optical information with surface features on a submicron scale. While cathodoluminescence mapping of $Al_{0.5}Ga_{0.5}N$ has previously been performed in high vacuum,[14] we were able to investigate the luminescence properties at a higher magnification where the charging effects are more pronounced. Using this technique, we observe that the miscut of the substrate has a great influence on the surface morphology and compositional inhomogeneity of the $Al_{0.5}Ga_{0.5}N$ buffer

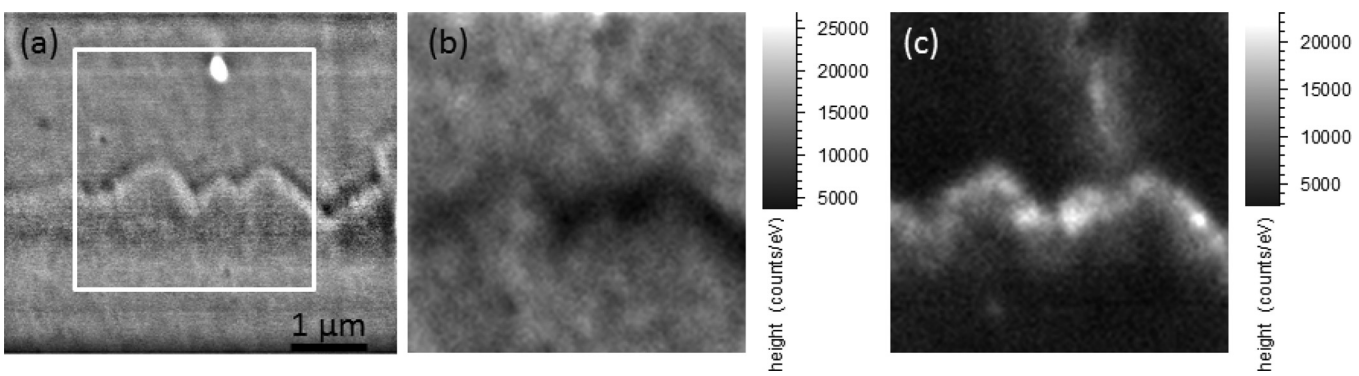


FIG. 4. SE image (a) and fitted $3 \times 3\ \mu m^2$ CL intensity maps of the 4.54 eV peak (b) and the 4.41 eV peak (c) of sample B.

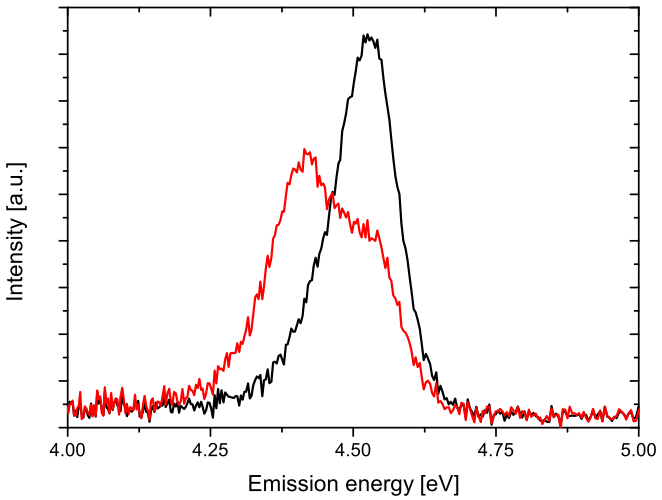


FIG. 5. CL spectra of sample B acquired in an area without step bunches (black) and centred on a step bunch (red).

layer. For the growth of an active region on top of the high miscut sample, the step edges and the higher GaN incorporation have to be taken into account as this reduces the effective absorption edge of the buffer layer. For the growth on the low miscut sample, the effect of the different domains has to be understood in order to prevent compositional inhomogeneity in the active zone and a resulting broadening of the emission band.

We acknowledge funding from the Engineering and Physical Sciences Research Council of the UK (Grant No. EP/I029141/1) and Science Foundation Ireland (Grant Nos. 10\IN.1\I2993 and 07\EN\E001A). T.C.S. acknowledges the Irish Research Council for his postdoctoral fellowship. This work was conducted under the framework of the Irish Government's Programme for Research in Third Level Institutions Cycle 4 and 5, National Development Plan 2007–2013 with the assistance of the European Regional Development Fund "INSPIRE." Access to the data underpinning the research published in this paper can be requested by contacting the corresponding author.

[1]R. W. Martin, P. R. Edwards, K. P. O'Donnell, M. D. Dawson, C.-W. Jeon, C. Liu, G. R. Rice, and I. M. Watson, Phys. Status Solidi A **201**, 665 (2004).
[2]J. Christen, M. Grundmann, and D. Bimberg, J. Vac. Sci. Technol., B **9**, 2358 (1991).
[3]P. R. Edwards, R. W. Martin, K. P. O'Donnell, and I. M. Watson, Phys. Status Solidi C **0**, 2474 (2003).
[4]D. Drouin, A. R. Couture, D. Joly, X. Tastet, V. Aimez, and R. Gauvin, Scanning **29**, 92 (2007).
[5]P. R. Edwards, L. K. Jagadamma, J. Bruckbauer, C. Liu, P. Shields, D. Allsopp, T. Wang, and R. W. Martin, Microsc. Microanal. **18**, 1212 (2012).
[6]J. Tersoff, Y. H. Phang, Z. Zhang, and M. G. Lagally, Phys. Rev. Lett. **75**, 2730 (1995).
[7]H. Lin, Y. Chen, T. Lin, C. Shih, K. Liu, and N. Chen, J. Cryst. Growth **290**, 225 (2006).
[8]J. Gong, W. Liao, S. Hsieh, P. Lin, and Y. Tsai, J. Cryst. Growth **249**, 28 (2003).
[9]Y. Koide, N. Itoh, N. Sawaki, and I. Akasaki, Jpn. J. Appl. Phys., Part 1 **27**, 1156 (1988).
[10]M. A. Khan, M. Shatalov, H. P. Maruska, H. M. Wang, and E. Kuokstis, Jpn. J. Appl. Phys., Part 1 **44**, 7191 (2005).
[11]D. Zhao, D. Jiang, J. Zhu, Z. Liu, S. Zhang, H. Yang, U. Jahn, and K. Ploog, J. Cryst. Growth **310**, 5266 (2008).
[12]T. Y. Chang, M. A. Moram, C. McAleese, M. J. Kappers, and C. J. Humphreys, J. Appl. Phys. **108**, 123522 (2010).
[13]S. Keller, C. S. Suh, N. A. Fichtenbaum, M. Furukawa, Z. C. R. Chu, K. Vijayraghavan, S. Rajan, S. P. DenBaars, J. S. Speck, and U. K. Mishra, J. Appl. Phys. **104**, 093510 (2008).
[14]A. Knauer, V. Kueller, U. Zeimer, M. Weyers, C. Reich, and M. Kneissl, Phys. Status Solidi A **210**, 451 (2013).